Available online at www.sciencedirect.com

SciVerse ScienceDirect

Ceramics International 39 (2013) 7205–7210

CERAMICS INTERNATIONAL

www.elsevier.com/locate/ceramint

# Research on CBN/TiC composites Part1: Effects of the cBN content and sintering process on the hardness and transverse rupture strength

Shi-Yung Chiou[a], Shih-Fu Ou[a,b,c,*], Yu-Gou Jang[a], Keng-Liang Ou[b,c,d,**]

[a]*Department of Mold and Die Engineering, National Kaohsiung University of Applied Science, Kaohsiung 813, Taiwan*
[b]*Research Center for Biomedical Devices and Prototyping Production, Taipei Medical University, Taipei 110, Taiwan*
[c]*Graduate Institute of Biomedical Materials and Tissue Engineering, College of Oral Medicine, Taipei Medical University, Taipei 110, Taiwan*
[d]*Research Center for Biomedical Implants and Microsurgery Devices, Taipei Medical University, Taipei 110, Taiwan*

Received 28 December 2012; received in revised form 19 February 2013; accepted 19 February 2013
Available online 27 February 2013

**Abstract**

Cubic boron nitride/ titanium carbide (cBN/TiC) composites were fabricated by a two-step sintering process. The effects of cBN/TiC ratio and sintering process on the microstructure, densification and mechanical properties of the cBN/TiC composites were studied. The results showed that the composite with a cBN/TiC ratio of 2:1 prepared by the two-step sintering exhibited the highest hardness. In addition, the two-step sintering could improve the hardness by inhibiting grain growth and could promote the transverse rupture strength by suppressing by-products formation.


*Keywords:* A. Sintering; B. Composites; D. Nitrides; E. Biomedical applications; Wear resistant

## 1. Introduction

The hardness and thermal conductivity values of cubic boron nitride (cBN) are second only to diamond. In addition, as compared to diamond, cBN is more thermally stable and less reactive with iron [1]. These characteristics enable cBN to be widely applied to cutting tools for hardened steel, cast iron and other ferrous alloys [2].

However, sintering high-density cBN is difficult owing to the predominantly covalent bonding [3] and low diffusion rate of boron and nitrogen [4–6]. Thus, a process comprising high pressures and high temperatures is necessary to fabricate completely densified cBN [7]. However, at high temperature, the structure of BN can transform from cubic to hexagonal [4–6].

Recently, many studies have focused on choosing suitable binders to sinter cBN at temperatures in the range 1200–1500 °C [8]. Metallic elements, such as, Al, Co and Ni [9,10] have been proposed that improve sintering. However, the metallic binders with low melting points are not suitable for high-temperature applications. Accordingly, ceramic binders such as TiC, TiN and $Al_2O_3$ have been developed for improving the mechanical properties of cBN compacts [11,12]. Among such binders, TiC has excellent chemical affinity with cBN. However, the typical sintering temperature for cBN/TiC composites is 1400–1600 °C [13] which causes grain overgrowth and deteriorates the mechanical strength. Furthermore, previous studies have indicated that during sintering, the by-products, $TiB_2$ is frequently found, which is brittle and could decrease the bond strength between TiC and cBN grains [14]. Consequently, maintaining a fine grain structure while simultaneously avoiding by-products formation during densification is required.

In this study, cBN/TiC composites were prepared by the two-step sintering process. The effects of cBN/TiC ratio and the sintering process on the densification, mechanical

*Corresponding author at: Taipei Medical University, No.250, Wu-hsing St., Taipei 11031, Taiwan. Tel.: 886 2 2736 1661x5100; fax: 886 2 2736 2295.
**Corresponding authors.
*E-mail address:* m9203510@gmail.com (S.-F. Ou), klou@tmu.edu.tw (K.-L. Ou).

0272-8842/$ - see front matter © 2013 Elsevier Ltd and Techna Group S.r.l. All rights reserved.
http://dx.doi.org/10.1016/j.ceramint.2013.02.066

properties, and microstructure of the cBN/TiC compacts were studied.

## 2. Experimental procedure

### 2.1. Sample compaction and sintering

Commercial cBN powder with an average particle size of 325 mesh and TiC powder with an average particle size of 3 μm were used. The cBN particles were coated by Ni for enhancing sintering ability. Composites with different cBN/TiC molar ratios of 2:1, 1:1, and 1:2 were prepared by wet milling in anhydrous alcohol for 3 h. Then, the isopropyl alcohol was removed before molding. The powders were pressed to 200 MPa for 1 min into green compacts. Pressing was followed by the consolidation of the green compacts by ambient pressure sintering performed under $10^{-3}$–$10^{-4}$ KPa using a vacuum furnace. The three sintering schedules are shown in Fig. 1. In the traditional sintering process 1 and 2, the samples were maintained at 1400 °C for 1 h and 2 h, respectively. For the two-step sintering, the sintering temperature was first increased to 1400 °C, and then decreased to 1250 °C; the samples were maintained at 1250 °C for 20 h. The samples with different cBN/TiC molar ratio sintered by various processes are denoted as 2:1–1, 2:1–2, 2:1–S, 1:1–1, 1:1–2, 1:1–S, 1:2–1, 1:2-2, and 1:2–S, where "S" denotes the two-step sintering process.

### 2.2. Characteristics of sintered compacts

The porosity of the sintered compacts was measured by Archimedes' method. The Vickers' hardness of the compacts was measured by using a hardness tester (MVK-H1, Meter-Mitutoyo, Japan)). Indentations were performed on polished surfaces at a test load of 300 N with an indentation time of 15 s. In this study, six samples for each sintering process were fabricated to obtain an average relative density and hardness. The transverse rupture strength (TRS) was determined by a three-point bending test according to JIS R1601 using a universal testing machine (SHIMADUZ UH-1) at a loading of 0.5 mm/min. The specimens were 40 × 4 × 3 mm in size.

### 2.3. Microstructures of sintered compacts

The different phases of the sintered compacts were characterized by powder X-ray diffractometry (XRD) (Model 2200, Rigaku Co., Tokyo, Japan). The sintered compacts were initially ground to a fine powder in isopropyl alcohol prior to laying them flat onto a glass sample holder. Monochromatic Cu Kα radiation was used at operating values of 40 kV and 30 mA. The XRD data were collected over a $2\theta$ range of 20–40° with a step size of 0.04°/step and a count time of 5 s. The etched microstructure was examined using scanning electron microscopy (SEM, Model JSM, JEOL Co., Tokyo, Japan). Transmission electron microscopy (TEM, Model JEM2100, JEOL Co., Tokyo, Japan) observation was used to characterize the unknown phases of the compacts.

## 3. Results and discussion

### 3.1. Characteristics of the cBN/TiC composites

Fig. 2 shows the hardness of the cBN composites. In a comparison of the hardness of composites with different ratios of cBN and TiC, higher hardness was observed with higher cBN content. For the composites with the same ratio of cBN/TiC, the composites fabricated by the two-step sintering process had the higher hardness than those prepared by the single sintering process. Previous studies have indicated that the mechanical properties of the sintered compact generally depended on the density, grain size and phase composition of the sintering compact [15,16]. With regard to the porosity of the composites, Fig. 3 shows that through the porosity of the composites

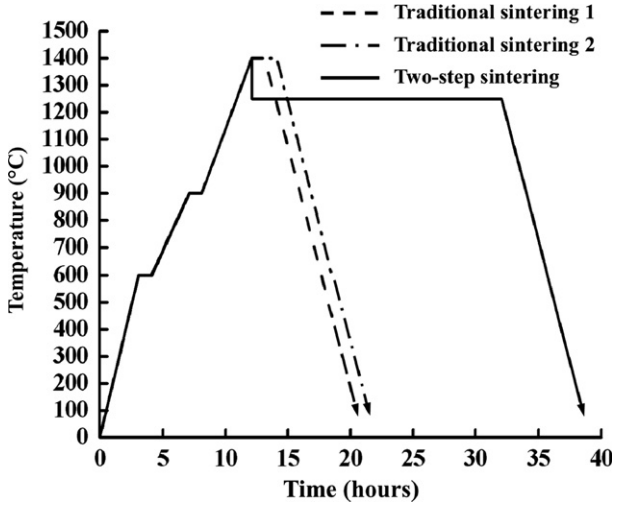


Fig. 1. Three types of sintering schedules.

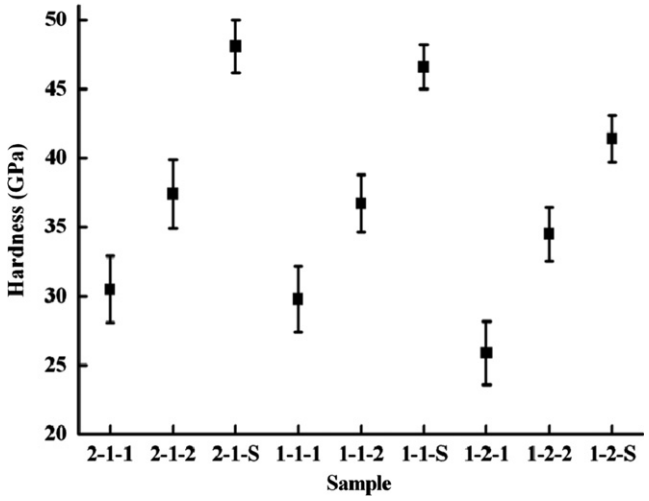


Fig. 2. The hardness of sintered composites.

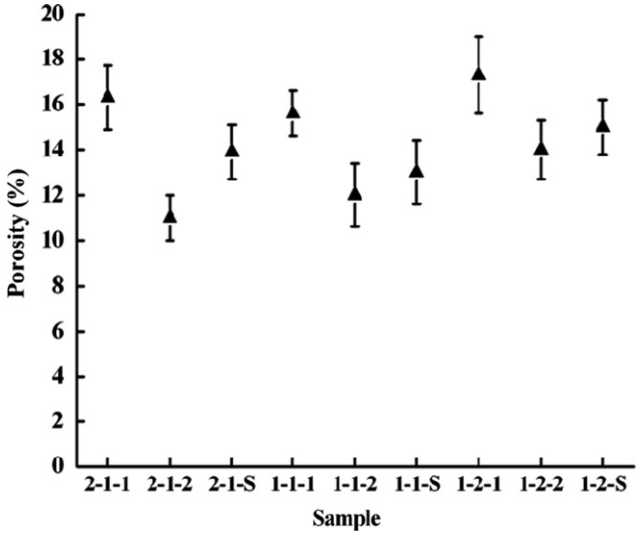


Fig. 3. The porosity of sintered composites.

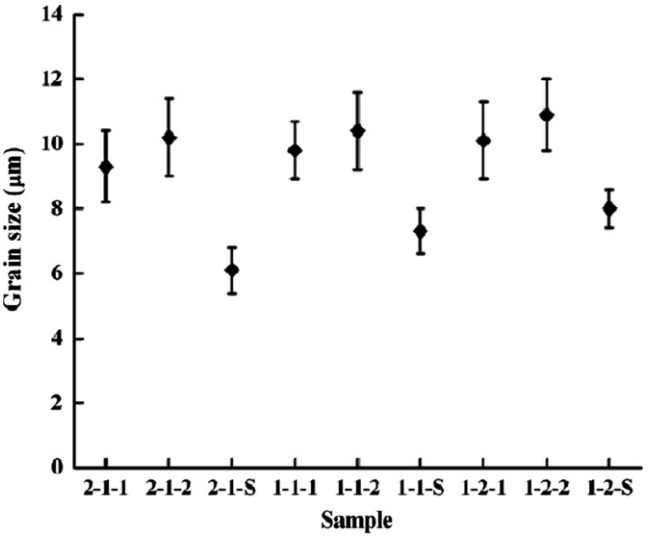


Fig. 4. The grain size of sintered composites.

was greatly affected by the sintering parameters, it was only slightly affected by the cBN/TiC ratio. Densification is a process of eliminating the pores along the grain boundaries that are introduced during green compact fabrication. Hence, a high temperature or a long sintering process can effectively reduce the porosity of a sintered compact. However, grain boundaries move faster than pores; therefore, isolated pores remain within the grain interior, thereby limiting the ability to achieve the maximum density even after sintering for a long periods of time or at high temperatures. Fig. 4 shows the grain size of the composites. The two-step sintering process significantly decreased the grain size of the composites. By comparing Figs. 2–4, the relationship between hardness, porosity, and grain size can be found. For example, 2–1–2 exhibited a higher hardness than 2–1–1 because it possessed less porosity. On the other hand, although 2–1–S had a higher porosity than 2–1–2, it had a higher hardness owing to its smaller grain size.

Fig. 5 shows the TRS of the sintered composites. The composites with a cBN/TiC ratio of 1:2 exhibited a higher TRS than those with rations of 2:1 and 1:1, which indicates that using TiC as a matrix can significantly improve the TRS. Among all the samples, 1–2–S had the highest TRS, which can be attributed to the small grain size. Generally, the TRS of sintered compacts depends on both the size and number of initial flaws (pores) and grain size [17], and the TRS appears to decrease with increasing grain size. Furthermore, cBN/TiC composites exhibit a higher TRS in comparison with the cBN bound by the bronze powder as reported by Kir [18], which suggests that TiC bonds well with cBN.

### 3.2. Microstructures of the cBN/TiC composites

Fig. 6 (a), (c), (e) and (g) show the SEM micrographs of 1:2–S, 1:2–2, 2:1–S and 2:1–2, respectively. In all the samples, the dark phase is cBN and the gray phase is TiC. Fig. 6(b), (d), (f) and (h) show the surface morphology of TiC in 1:2–S, 1:2–2, 2:1–S, and 2:1–2 after etching, respectively. In a comparison of 1:2–S and 1:2–2, the grain size of TiC in 1:2–S is found to be significantly smaller than that in 1:2–2, as shown in Fig. 6(b) and (d). Also, a comparison of Fig. 6(f) and (h) shows that 2:1–S has a smaller grain size than 2:1–2.

Fig. 7(a) shows the XRD patterns of the composites with a cBN/TiC ratio of 1:2 sintered by various processes. For 2–1–1, the peaks of cBN, TiC, TiB, and Ti($C_xN_y$) were identified in the XRD patterns. The formation of Ti($C_xN_y$) is considered to result from a reaction of TiN with TiC. Previous studies have reported that TiN is formed at approximate 1000 °C [19,20] and that it continues to react with TiC to form Ti ($C_xN_y$) [21]. However, the Ti($C_xN_y$) was not found in 1:1–1 and 1:2–1 because the content of cBN were too low to form TiN. Also, the TiN did not

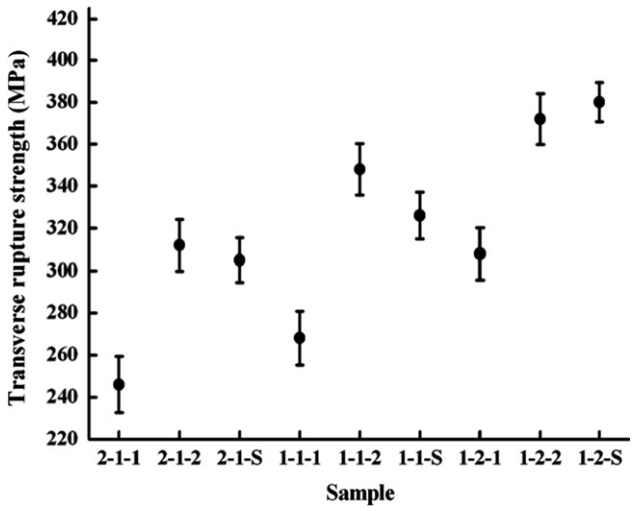


Fig. 5. The transverse rupture strength of sintered composites.

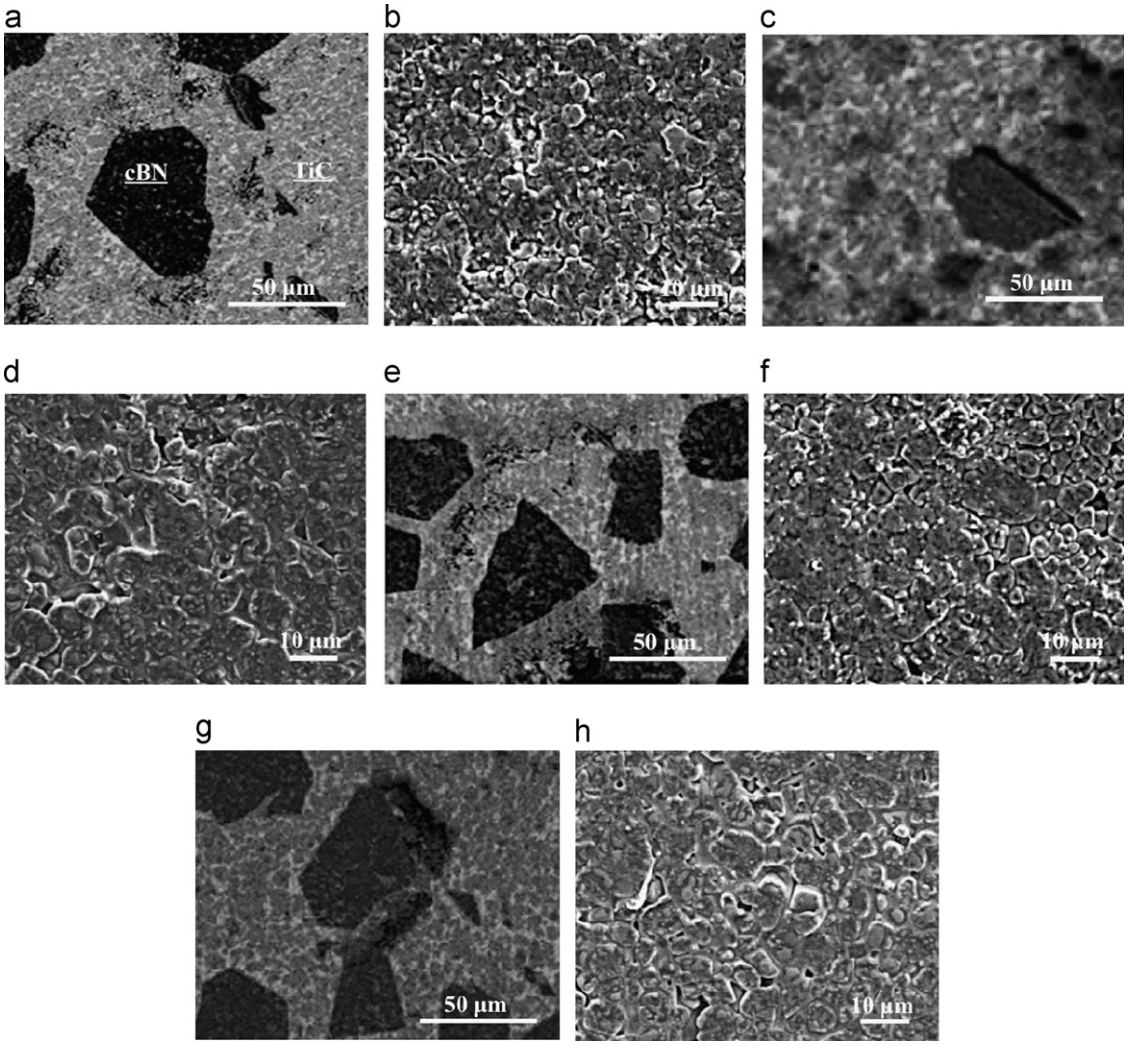


Fig. 6. The SEM micrographs of (a) the 1:2–S, (c) 1:2–2, (e) 2:1–S and (g) 2:1–2 after polishing. (b), (d), (f) and (h) is the SEM micrograph of the TiC in the 1:2–S, 1:2–2, 2:1–S and 2:1–2 after etching.

appear in the composites with cBN/TiC ratios of 1:1 and 1:2 even after the composites were sintered for a long duration. Therefore, the number of N atoms is crucial for the formation of TiN and Ti($C_xN_y$). A previous study reported that TiB and $TiB_2$ were found over a wide range of sintering temperatures and pressures [22]. According to the free energy of the products, TiB (−36 kcal/mole) and $TiB_2$ (−59.9 kcal/mole) form at 1400 °C, and $TiB_2$ is more stable than TiB. However, during sintering, the B atoms gradually diffuse from cBN, preferentially forming TiB. Furthermore, TiB, regarded as an intermediate phase that forms in the earlier stages of sintering, is expected to transform to the final product $TiB_2$.

For 2:1–2, except for the peaks of cBN and TiC, the peaks of $TiB_2$, $Ti_2N$, $Ti_xNi_y$, $Ti_2Ni$, and $Ni_4B_3$ appeared in the XRD patterns, as shown in Fig. 7(a). These results agree with those reported in other studies. For example, Zhang indicated that TiN is formed at about 1000 °C, whereas $TiB_2$ occurred above 1200 °C when Ti reacts with BN at the elevated temperatures [19]. Furthermore, $TiB_2$ is formed by a reaction of $Ti_2N$ or TiC with cBN at 1600 °C [22,23]. The formation of $Ti_xN_y$ locally increased the ratio of Ni and Ti, leading to the formation of a low-temperature liquid according to the Ti–Ni phase diagram [24]. The low-temperature liquid can enhance the inter-diffusion of particles, and therefore, improve the densification of 2:1–2. For 2:1-S, the peaks of cBN, TiC, and $TiB_2$ were found in the XRD patterns, as shown in Fig. 7(a).

Fig. 7(b) shows the XRD patterns of the composites with a cBN/TiC ratio of 1:2. The byproduct TiB was presented in 1:2–1 and $TiB_2$ appeared in both 1:2–2 and 1:2–S. Similar to the composites with a cBN/TiC ratio of 2:1, 1:2–S contained lower content of $TiB_2$ than 1:2–2, which can be attributed to the low-temperature sintering. The presence of $TiB_2$ is harmful to the mechanical strength of the composites because $TiB_2$ is brittle and will deteriorate the bonding strength between TiC and cBN. In the present study, the TRS of a compact depends on its porosity and composition. For example, on comparing the porosity (Fig. 3) and TRS (Fig. 5) of 1:2–2 and 1:2–S, 1:2–S was found to have a slightly lower density but a higher

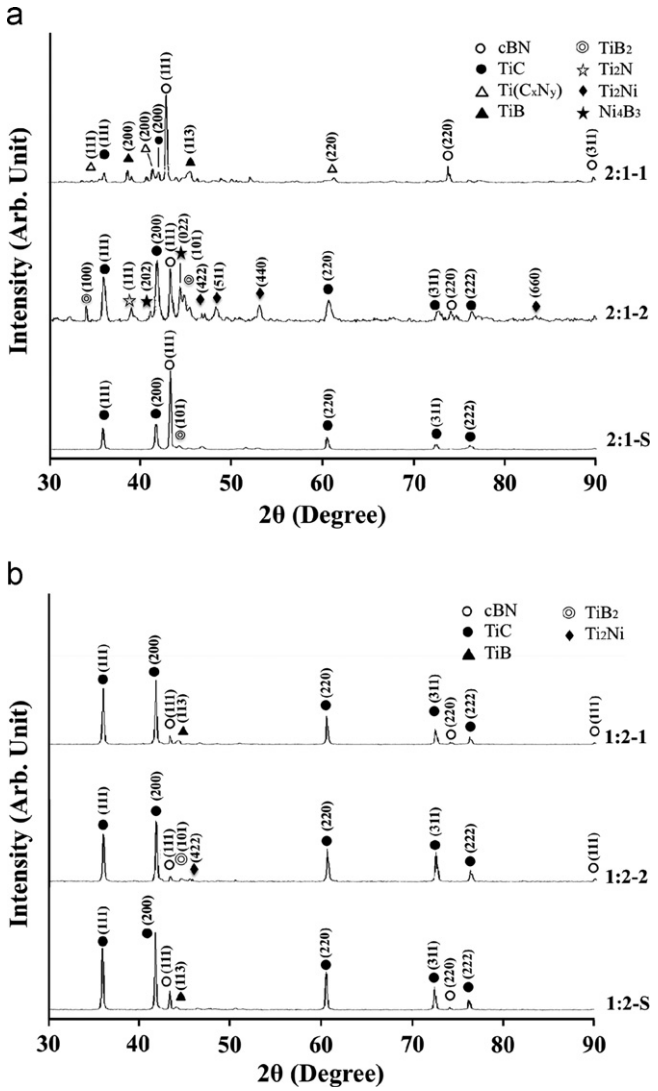


Fig. 7. The XRD patterns of composites with cBN–TiC ratio of (a) 2:1 and (b) 1:2.

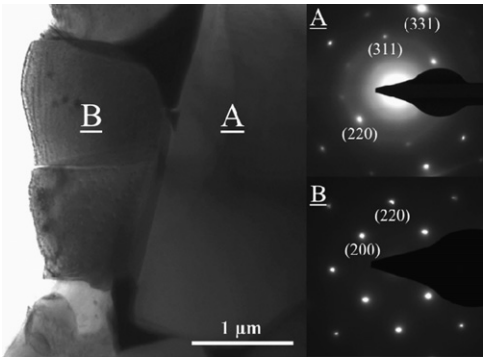


Fig. 8. The TEM micrograph of the 2:1–S.

TRS than 1:2–2. This is because the content of byproducts was greater in 1:2–2 than 1:2–S.

Fig. 8 shows the bright-field TEM micrograph of 2:1–S. Fig. 8 also depicts the selected area diffraction pattern (SADP) of an area denoted as A, revealing that A is a cBN grain. Area B was identified as a TiC gain, which is in close contact with the cBN grain. The dark-contrast lines observed in the TiC grain were considered to be thickness fringes. Although $TiB_2$ was found between the TiC and cBN [13] and also detected by the XRD analysis in the present study, $TiB_2$ was not observed in the TEM micrograph (Fig. 8). Consequently, $TiB_2$ was formed only locally in the composite.

## 4. Conclusions

This study prepared cBN/TiC composites by a two-step sintering process. The effects of sintering process and cBN/TiC ratio on the microstructure, densification and mechanical properties were investigated. The composite with a cBN/TiC ratio of 2:1 had a combined hardness of 4905 Hv and a TRS of 334 MPa. Compared with conventional sintering, the two-step sintering process improved the hardness and TRS owing to grain growth and the inhibition of byproducts of the composites.

## Acknowledgments

The authors would like to thank researcher Kuang-Kuo Wang for TEM identification.

## References

[1] S. Goel, X. Luo, R.L. Reuben, W.B. Rashid, Replacing diamond cutting tools with CBN for efficient nanometric cutting of silicon, Materials Letters 68 (2012) 507–509.
[2] R.H. Wentorf, R.C. DeVries, F.P. Bundy, Sintered superhard materials, Science 208 (4446) (1980).
[3] T.K. Harris, E.J. Brookes, C.J. Taylor, The effect of temperature on the hardness of polycrystalline cubic boron nitride cutting tool materials, International Journal of Refractory Metals and Hard Materials 22 (2–3) (2004) 105–110.
[4] F.P. bundy, R.H. Wentorf, Direct transition among the allotropic forms of boron nitride at high pressure and temperature, Journal of Chemical Physics 38 (5) (1963) 1144–1149.
[5] F.R. Corrigan, F.P. Bundy, Direct transitions among the allotropic forms of boron nitride at high pressures and temperatures, Journal of Chemical Physics 63 (1975) 3812–3820.
[6] V.L. Solozhenko, V.Z. Turkevich, W.B. Holzapfel, hBN+cBN equilibrium line calculated from experimental data on the cBN-to-hBN transformation to 1.4 GPa, High Temperature Research 16 (1999) 179–185.
[7] T. Taniguchi, M. Akaishi, S. Yamaoka, Sintering of cubic boron nitride without additives at 7.7 GPa and above 2000 8C, Journal of Materials Research 14 (1) (1999) 162–169.
[8] R. Riedel, Handbook of Ceramic Hard Materials, Wiley-VCH, Weinheim, 2000.
[9] E. Benko, P. Klimczyk, S. Mackiewicz, T.L. Barr, E. Piskorska, cBN–$Ti_3SiC_2$ composites, Diamond and RelatedMaterials 13 (3) (2004) 521–525.
[10] Sumitomo Electrical Industries Ltd., US Patent 4 334 063, 1982.
[11] M. Hotta, T. Goto, Densification and microstructure of $Al_2O_3$–cBN composites prepared by spark plasma sintering, Journal of the Ceramic Society of Japan 116 (6) (2008) 744–748.
[12] H. Zhang, S. Gu, J. Yi, Fabrication and properties of Ti(C,N) based cermets reinforced by nano-cBN particles, Ceramics International 38 (2012) 4587–4591.

[13] E. Benkoa, T.L. Barr, S. Hardcastle, E. Hoppe, A. Bernasik, J. Morgiele, XPS study of the cBN–TiC system, Ceramics International 27 (2001) 637–643.
[14] M. Hotta, T. Goto, Spark plasma sintering of TiN-cubic BN composites, Journal of the Ceramic Society of Japan 118 (2) (2010) 137–140.
[15] K.-T. Chu, S.-F. Ou, S.-Y. Chen, S.-Y. Chiou, H.-H. Chou, K.-L. Ou, Research of phase transformation induced biodegradable properties on hydroxyapatite and tricalcium phosphate based bioceramic, Ceramics International 39 (2) (2013) 1455–1462.
[16] S.-F. Ou, S.-Y. Chiou, K.-L. Ou, Phase transformation of hydroxyapatite decomposition, Ceramics International, http://dx.doi.org/10.1016/j.ceramint.2012.1010.1221.
[17] J. Seidel, N. Claussen, J. Rödel, Reliability of alumina ceramics: effect of grain size, Journal of the Europea Ceramic Society 15 (1995) 395–404.
[18] D. Kır, S. Islak, H. Çelik, E. Çelik, Effect of the cBN content and sintering temperature on the transverse rupture strength and hardness of cBN/diamond cutting tools, Science of Sintering 44 (2012) 235–243.
[19] G.J. Zhang, Z.Z. Jin, X.M. Yue, TiN-$TiB_2$ composites prepared by reactive hot pressing and effects of Ni addition, Journal of American Ceramic Society 78 (10) (1995) 2831–2833.
[20] T. Watanabe, H. Yamamoto, K. Shobu, T. Sakamoto, Factors affecting the porosity and bending strength of Ti(CN)–$TiB_2$ materials, Journal of American ceramic society 71 (4) (1988) 202–204.
[21] J. Li, F. Li, K. Hu, Y. Zhou, Formation of TiB2/TiN/Ti(CN) nanocomposite powder via high-energy ball milling and subsequent heat treatment, Journal of Alloys and Compounds 334 (2002) 253–260.
[22] E. Benko, J.S. Stanisław, B. Królicka, A. Wyczesany, T.L. Barr, cBN–TiN, cBN–TiC composites: chemical equilibria, microstructure and hardness mechanical investigations, Diamond and Related Materials 8 (1999) 1838–1846.
[23] F. Ueda, M. Yageta, I. Tajima, Microstructure and mechanical properties of cBN–TiN composites, Journal of Hard Materials 2 (1991) 233–243.
[24] Alloy Phase Diagrams, ASM Handbook, Vol. 3, ASM International, Materials Park, OH, 1992.